Intervertebral Disc Segmentation Using Machine Learning

Author

IQRA SAEED

00000204117

Supervisor

Dr. Syed Omer Gilani

DEPARTMENT OF BIOMEDICAL ENGINEERING AND SCIENCES

SCHOOL OF MECHANICAL & MANUFACTURING ENGINEERING

NATIONAL UNIVERSITY OF SCIENCES AND TECHNOLOGY

ISLAMABAD, PAKISTAN

JUNE 2021

Intervertebral Disc Segmentation Using Machine Learning

Author

IQRA SAEED

00000204117

A thesis submitted in partial fulfillment of the requirements for the degree of

MS Biomedical Science

Thesis Supervisor:

Dr. Syed Omer Gilani

Thesis Supervisor's Signature: _____

DEPARTMENT OF BIOMEDICAL ENGINEERING AND SCIENCES

SCHOOL OF MECHANICAL & MANUFACTURING ENGINEERING

NATIONAL UNIVERSITY OF SCIENCES AND TECHNOLOGY,

ISLAMABAD, PAKISTAN

JUNE 2021

THESIS ACCEPTANCE CERTIFICATE

It is certified that the final copy of MS Thesis written by Ms. Iqra Saeed (Registration No. 00000204117), of SMME (School of Mechanical and Manufacturing Engineering) has been vetted by undersigned, found complete in all respects as per NUST statutes / regulations, is free of plagiarism, errors and mistakes and is accepted as partial fulfillment for award of MS/MPhil Degree. It is further certified that necessary amendments as pointed out by GEC members of the scholar have also been incorporated in the thesis.

Signature: _____

Name of Supervisor: Dr. Syed Omer Gilani

Date: _____

Signature (HOD): _____

Date: _____

Signature (Principal): _____

Date: _____

MASTER THESIS WORK

We hereby recommend that the dissertation prepared under our supervision by: Iqra Saeed Regn no: 00000204117 Titled: "**Intervertebral Discs Segmentation Using Machine Learning**" be accepted in partial fulfillment of the requirements for the award of **MS Biomedical Science** degree.

(Grade _____)

<u>Examination Committee Members</u>

1. Name:___Dr. Umer Ansari_   Signature:_____

2. Name:__Dr. Jawad Aslam__   Signature:_____

Supervisor's name: <u>Dr. Syed Omer Gilani</u>   Signature:_____

Date:_____

_____   _____

Head of Department   Date

<u>COUNTERSINGED</u>

Date: _____   _____

Dean/Principal

Declaration

I certify that this research work titled "**Intervertebral Discs Segmentation Using Machine Learning**" is my own work. The work has not been presented elsewhere for assessment. The material that has been used from other sources has been properly acknowledged / referred.

Signature of Student
Iqra Saeed
00000204117

Plagiarism Certificate (Turnitin Report)

This thesis has been checked for Plagiarism. Turnitin report endorsed by Supervisor is attached.

Signature of Student

Iqra Saeed

Registration Number

00000204117

Signature of Supervisor

Copyright Statement

Acknowledgements

Abstract

Disc degenerative changes are the most common cause of lower back pain. Treatment for this acute or chronic pain is physiotherapy or spine surgical procedures. These procedures include laminectomy or discectomy in which affected discs are surgically treated (removed). And for this purpose, disc location, size and shape are the main prerequisites. Initially surgeons used to rely on manually segmented data by Radiologists. Machine learning has revolutionized the medical field with the ability of making computers learn the common trends about disease patterns and predict pathological diagnosis in a very robust way. Many methods of machine learning have been developed for localization and segmentation of different anatomical structures, tumors or other pathologies and also used for histological studies of human body tissues. Moreover, several advancements in machine learning has increased the accuracy of diagnosis like in deep learning, densely connected convolutional neural networks have proved to be the accurate way of segmentation with high dice score The main pupose of this study is to segment the intervertebral discs automatically using densely connected network integrated into U-Net model in order to make computer aided diagnosis and surgical planning using MRI images of different modalities. The data set used is IVDM3Seg and taken from MICCAI 2018 challenge provided at grandchallenge.org. Segmentation models are trained on different MRI modalities given in the dataset and finally all the trained models are ensembled to get a satisfactory output. Final model resulted in 99.1% dice accuracy score which came out to be far better than previously used techniques.

Key Words: *Disc degenerative changes, Computer aided diagnosis, Automatic Segmentation, MRI modalities, MICCAI 2018 challenge, U-Net model training*

Table of Contents

List of Figures

List of Tables

List of Acronyms

MRI	Magnetic Resonance Imaging
CT	Computed Tomography
IVD	Intervertebral disc
ROI	Region of Interest
PDw	Proton Density Weighted
MEDIC	Multi Echo Data Image Combination
FCM	Fuzzy c means
RFCM	Robust FCM
CSF	Cerebrospinal Fluid
DSI	DICE similarity Index
CNN	Convolutional Neural Network
FCN	Fully Convolution Network
CRF	Conditional Random Field
HD	Hausdorff Distance
NIFTI	Neuroimaging Informatics Technology Initiative
RCNN	Region Based Convolutional Neural Network
MSD	Mean Surface Distance

1 CHAPTER 1: INTRODUCTION

1.1 Vertebral Column

Vertebral column or backbone is a flexible structure of support extending from base of skull to the lower back in human beings. It consists of 33 vertebrae with intervertebral discs between them and are joined together via intervertebral joints. These 33 vertebrae are divided in to five classes and named according to their position in the body. There are seven cervical, twelve thoracic, five lumbar, five fused sacral and four fused coccygeal vertebrae. A vertebra consists of a vertebral body, two transverse processes and a spinous process(Frost et al., 2019).
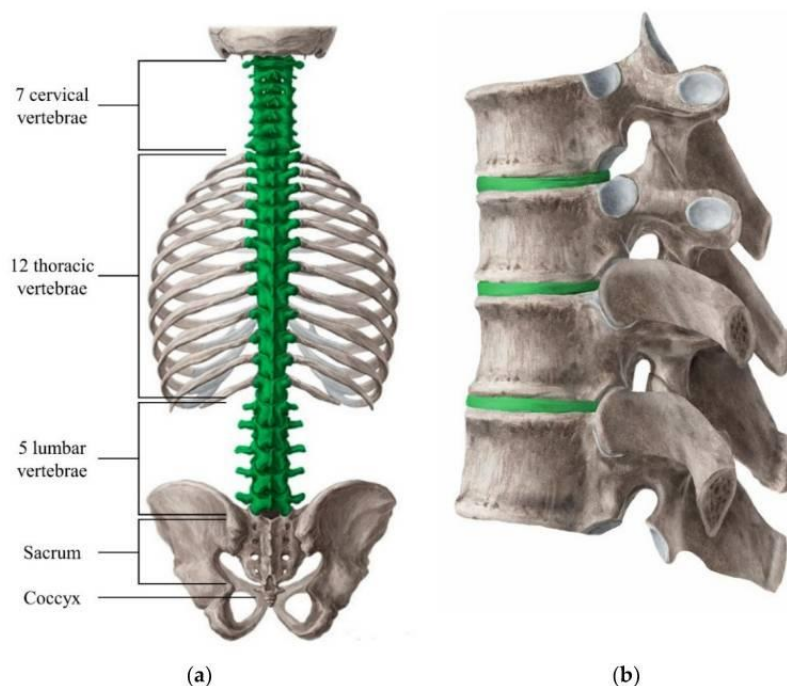
Figure 1 Vertebral Column: Adapted from (Frost et al., 2019)
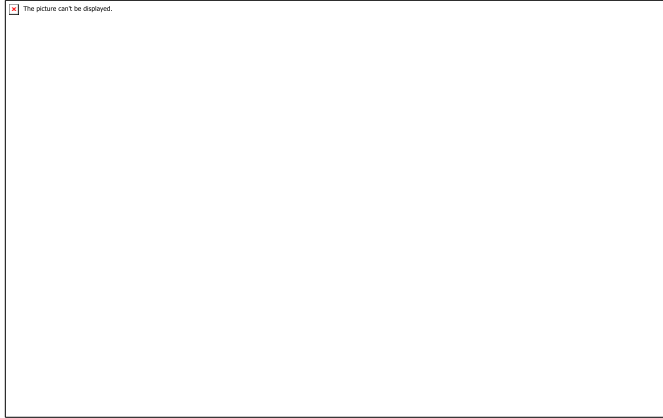
Figure 2 Structure of vertebral bodies. Adapted from (Chaturvedi et al., 2018)

Intervertebral discs are the soft cushions between vertebral bones which play hydro-mechanical role in human support and movement system. It consists of outer fibrocartilagenous structure made of collagen fibrils, called annulus fibrosus and inner gelatinous mass called nucleus pulposus which act as a shock absorbing structure(Ruiz Wills, 2015).
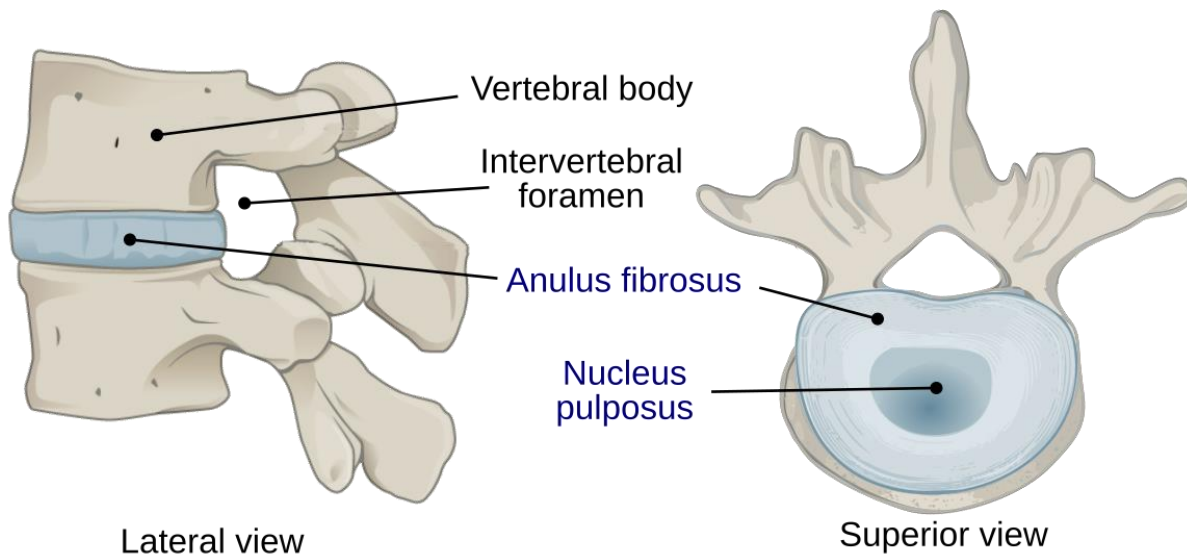
Figure 3 Intervertebral Disc Representation. Adapted from
https://en.wikipedia.org/wiki/Intervertebral_disc#/media/File:716_Intervertebral_Disk.svg

2

1.2 Disc Pathologies

With aging, discs begin to wear down causing disc degenerative disease(*The Proper Terminology for Reporting Lumbar Intervertebral Disk Disorders - PubMed*, n.d.). It occurs because of three reasons:

1. Injury to spine

2. Tears in the outer ring of the disc due to strenuous daily activities

3. Drying out of the disc with age

Unlike other tissues of the body, discs do not have sufficient blood supply to repair after injury so these start to deteriorate after any trauma leading to mild or severe symptoms like backache (Modic & Ross, 2007) and unilateral or bilateral radiculopathy.
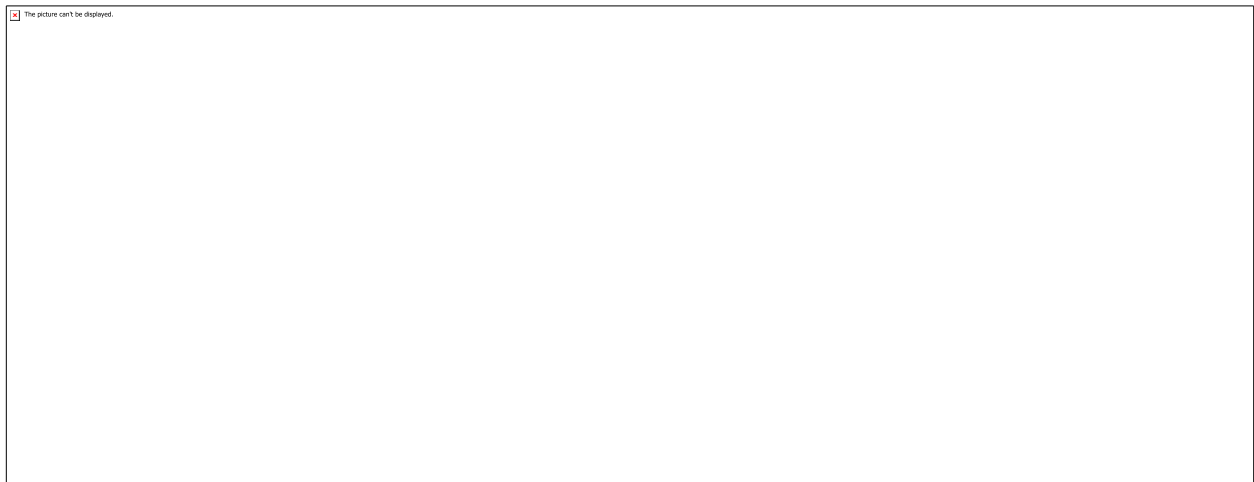
*Figure 4 Stages of IVD Degeneration Adapted from (*Can Stem Cells Help Reverse Degenerative Disc Disease?*, n.d.)*

1.3   Lumbar Vertebrae

There are five lumbar vertebrae, and these are biggest of all other vertebrae and their main function is to bear whole weight of the body and these allow certain movements like object lifting. They also provide protection to the spinal cord and nerves arising from it against any traumatic injury. There are many disorders that can affect the lumbar vertebrae and other vertebrae as well that can lead to different pathologies i.e. disc herniation, disc protrusion or extrusion which pressurize the spinal cord and cause severe pain. (Adams & Roughley, 2006).
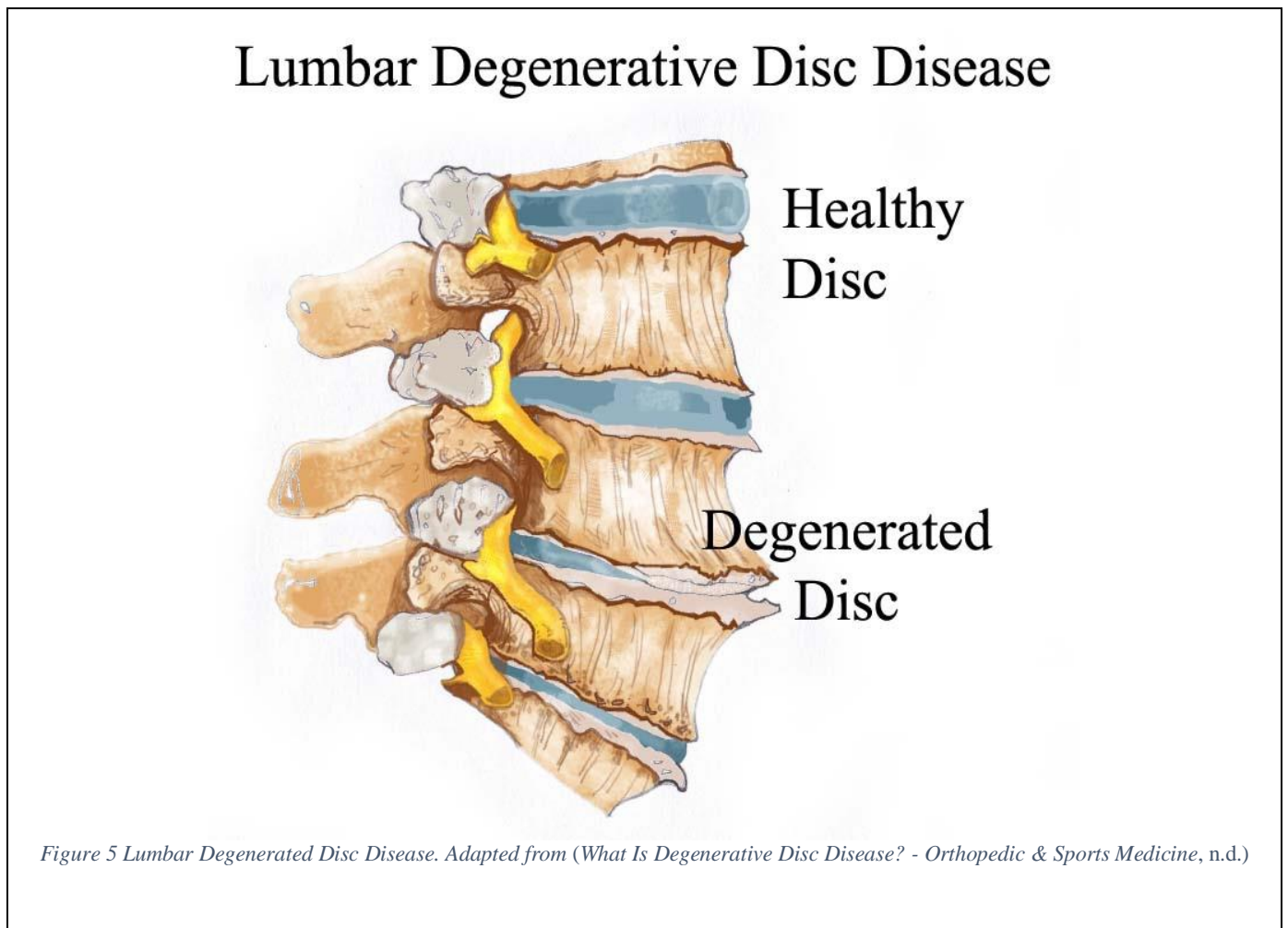
Figure 5 Lumbar Degenerated Disc Disease. Adapted from (What Is Degenerative Disc Disease? - Orthopedic & Sports Medicine, n.d.)

1.4   Different Diagnostic Modalities

For the diagnosis of these disorders, there are many imaging modalities like plain radiography (X-Rays), Computed Tomography (CT scanning) and Magnetic Resonance Imaging (MRI scanning). For tumor studies Nuclear Medicine Gamma Imaging Bone scans and Positron Emission Tomography (PET scanning) are also used.

X-RAY	CT SCAN	MRI
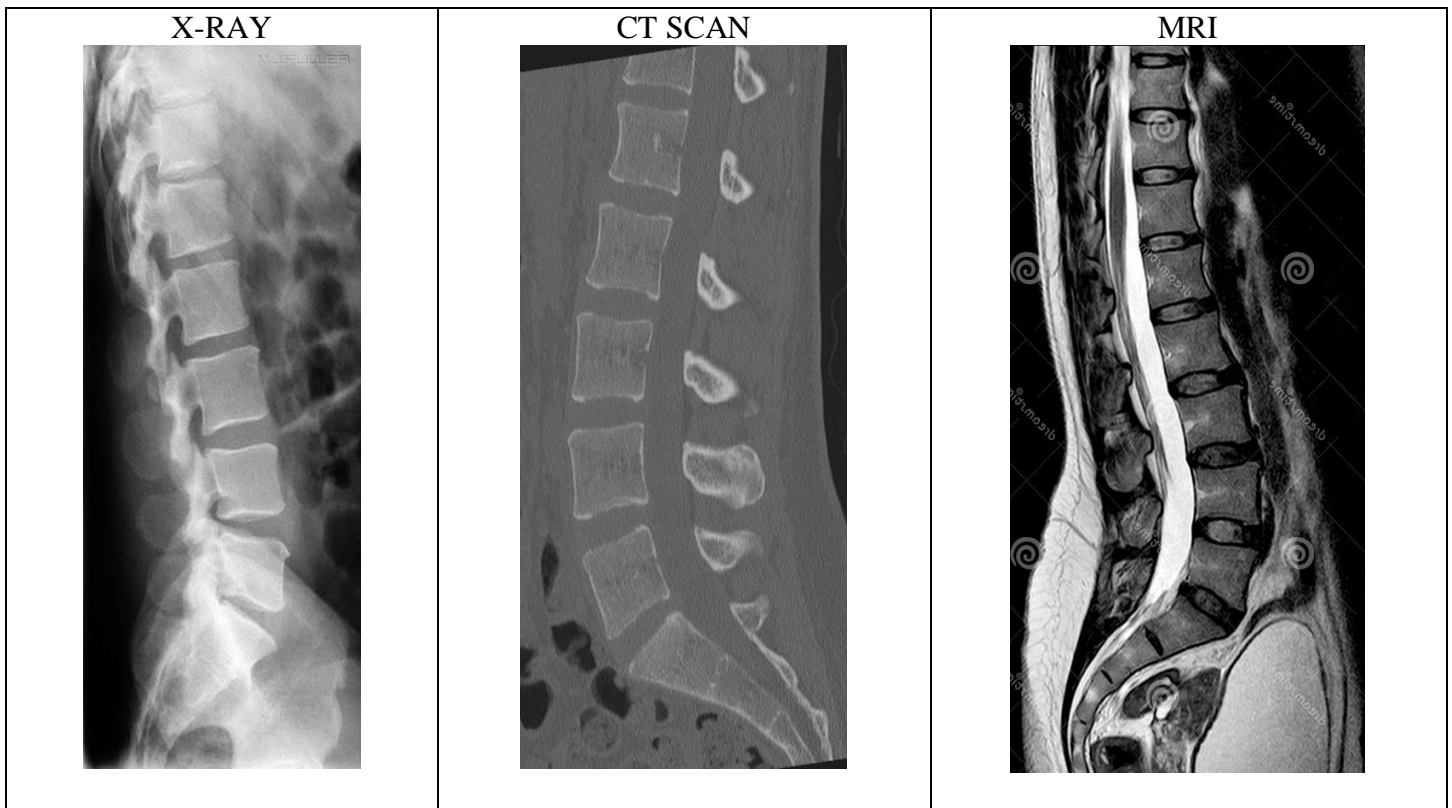
Figure 6 Different Modalities for Spine Imaging

All these modalities differ in their image acquisition methods and their anatomical appearance in the image differ as well. Image quality is described in terms of image resolution which is further defined by spatial resolution (difference between two closely spaced lines-minute details in the image) and contrast resolution (difference between shades of greys of two adjacent structures). Due to better image quality Magnetic Resonance Imaging is superior to other modalities (An et al., 2004) in diagnosing disc degenerative diseases because of its high contrast resolution and can

5

be acquired in different sequences which are basically different in shades of greys from each other for a better diagnosis of any abnormalities in bodily tissues. Although MRI is a costly and time consuming imaging modality and there is also restraint of different scanners with different parameters and variation in grey scale values.

1.5 Magnetic Resonance Imaging

MRI sequences work by exciting the hydrogen atoms of water and fat tissues in the body upon interaction with external magnetic field. And when these tissues relax, because of their different structures and bonds within molecules hydrogen proton of water and hydrogen in fat molecules relax and de-phase at different times giving different shades of greys which are called T1 and T2 sequences. Other sequences arise from these two (Broadhouse, 2019).
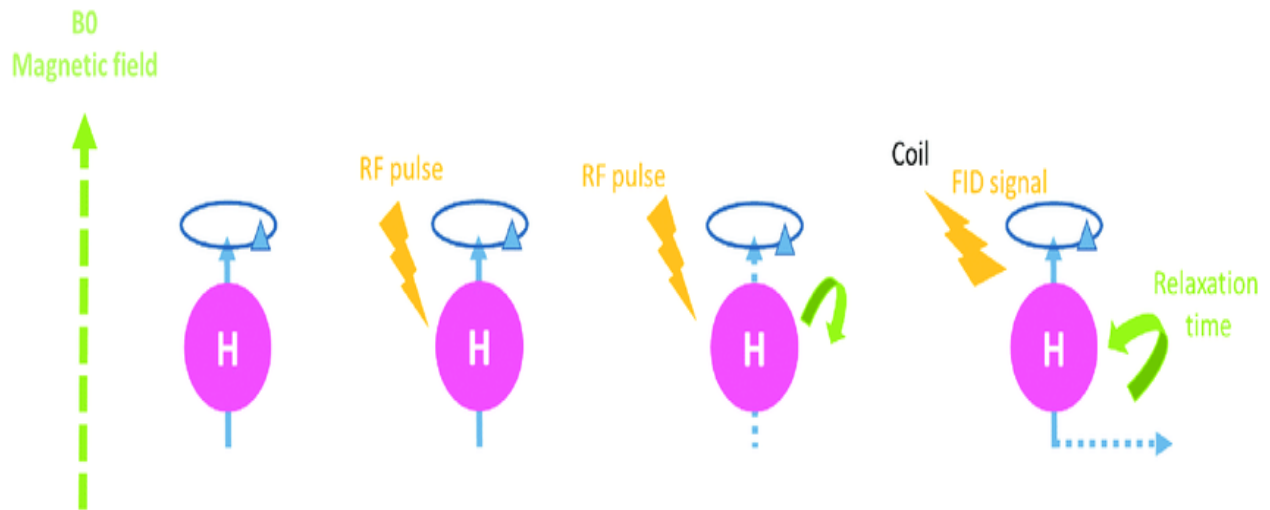
Figure 7 Schematic Representation of Working of an MRI. Adapted from(Schematic Representation of Magnetic Resonance Imaging Principles. (A)... | Download Scientific Diagram, n.d.)

1.5.1 T1 weighted sequence

After the excitation pulse, when spinning protons achieve almost 63% of their original magnetization state, they relax by releasing absorbed energy in the form of a signal. This is called

T1 relaxation time. This is also called spin-lattice relaxation time because the spinning protons give off their energy to the surrounding lattices. And all tissues relax at different times because of their different chemical bonds and at this time the signals from different tissues make up the T1 sequence (Pooley, 2005).

Fat: Fast realignment rate so it appears white

Water: Slow realignment rate so it appears dark

1.5.2 T2 weighted sequence

While protons are relaxing towards main magnetic field, meanwhile they also relax by dephasing from their aligned precession and differences in this dephasing of different protons in different tissues (fat, water etc.) make up the T2 sequence (Pooley, 2005).

Fat: intermediate bright

Water: bright
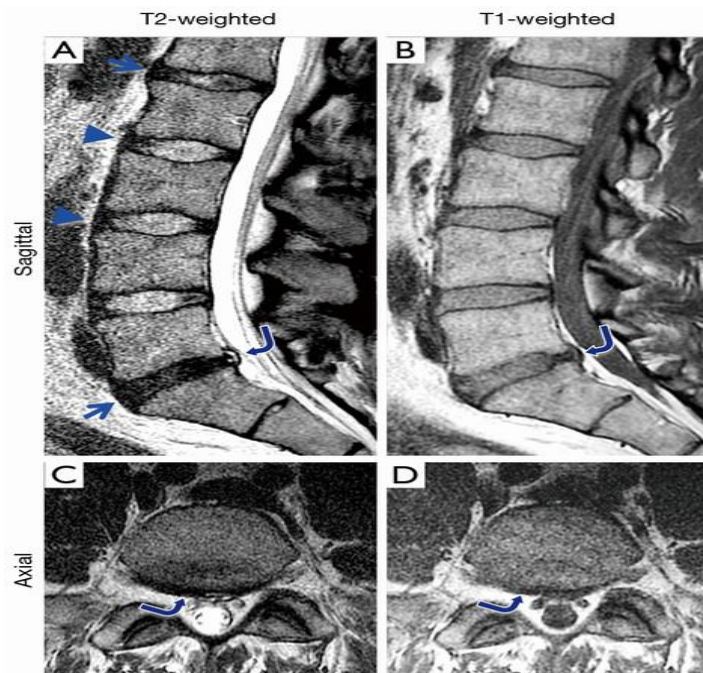
Figure 8 T1w versus T2w Sequences. Adapted from ((Hwang et al., 2016)

1.5.3 DIXON Sequences

Fat suppression is a common method used in T1w and T2w sequences to suppress the signal from adipose tissues or to detect the fat. Fat molecules have short relaxation times so it appears bright on MR images with high signal intensity which may be useful to identify lesions (van Vucht et al., 2019).

Fat suppression can be achieved in different ways. Dixon technique can be used for such purpose. In this technique fat and water molecules possess different precession rates.

As such, over time, they alternate their phase i.e. between being in phase and opposed phase. And then mathematically both phases can be combined while their acquisition being carried on in two ways giving four different contrasts:

1. In-phase = water + fat

2. Out of phase = water – fat

3. Fat only = In-phase - Out of phase = (water + fat) - (water - fat)

4. Water only = In-phase + Out of phase = (water + fat) + (water - fat)
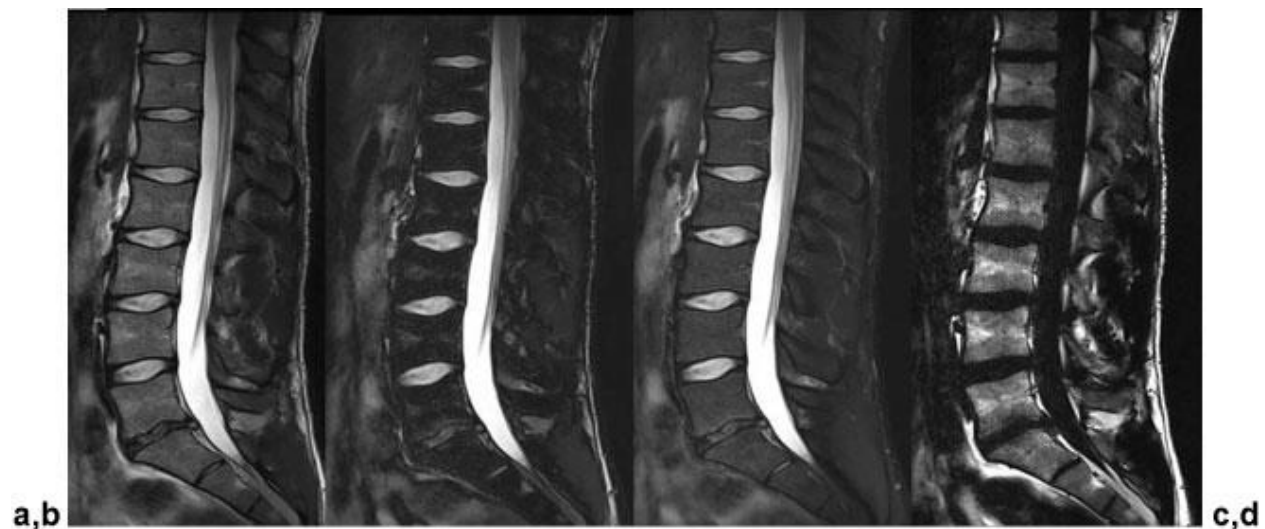
Figure 9 (a) In-phase image without fat suppression. (b) Out-of-phase image. (c) Water image (with fat suppression). (d) Fat image (with awater suppression. Adapted from (Guerini et al., 2015)

One T2-weighted acquisition leads to four reconstructed images mentioned above.

1.6   Need for Automatic Segmentation

As MRI is the modality of choice for diagnosing different spine conditions for its superiority over other modalities (An et al., 2004) due to good contrast resolution and no ionizing radiation are used in its acquisition. And with many advancements in the field of MRI many different sequences can be obtained using different parameters. The only drawback which comes here is the huge load of data which has become a burden on manual assessment of the pathologies, and it is very time consuming and prone to errors as well. So here comes the need of machine learning for automatic localization and segmentation of the affected area for making proper diagnosis prior to any treatment or surgical planning(*(PDF) AUTOMATIC SEGMENTATION OF CERVICAL SOFT TISSUE FROM MR IMAGES*, n.d.).

Deep Learning has achieved tremendous success in localizing and segmenting high-grade brain tumors and has made timely diagnosis and in time surgical resection of the affected area possible and added to the years in life. Similarly, localizing and segmenting degenerated intervertebral discs automatically saves the time and makes possible the early diagnosis of the degeneration and helps surgeons for their spinal procedures.

Instead of manual image analysis (Tsai et al., 2002) (Niemeläinen et al., 2008) (disc detection and segmentation) many semi-automatic and fully automatic methods have been employed.
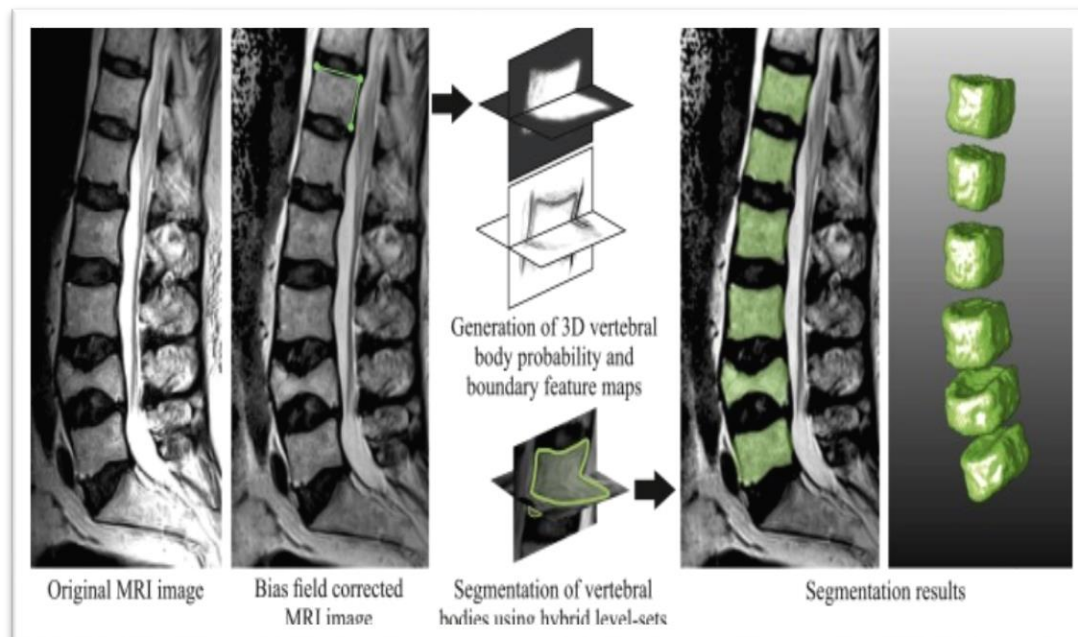
Figure 10 Automatic Segmentation of Vertebral Bodies Adapted from( )

Semi-automatic methods are less time consuming and efficient, but user variability exists, so these are not widely accepted. These also require interaction of user for three main purposes.

1. Initialization (ROI)
2. Processing by intervention or feedback response
3. Evaluation of the results for modification or repetition if required.

These methods include tumor cut methods (Hamamci et al., 2012) and classification methods. In fully automatic methods, there is no user interaction and artificial knowledge is used. Again, there are some challenges which make the segmentation difficult including.

1. Patient to patient variation in size and shape
2. Difference in MRI protocols and sequences

1.7   Thesis Overview

In this research an automated method of segmentation is developed using artificial knowledge of deep learning. Fully convolutional neural network is trained on MR images of different modalities and then tested later on. This study aims to achieve better results in segmenting the discs than the previously available studies.

2 CHAPTER 2: LITERATURE REVIEW

In this segment, methods that have been used previously for the purpose of segmentation of different bodily structures especially intervertebral discs of lumbosacral spine are briefly reviewed. To make computer aided diagnosis of the degenerated discs, their segmentation is a main pre-requisite that could help the clinicians for their future surgical and treatment planning. In clinical practice, radiologists usually localize and segment IVDs manually for the quantitative diagnosis of disc pathology (Violas et al., 2007). However, this way of segmentation is time consuming and depends on the expertise experience, which often leads to significant errors and variations occur in making the diagnosis. Many methods have been used in the past to segment intervertebral discs in semi-automatic and fully automatic way. Roberts et al. (Roberts et al., 1997) used watershed techniques to automatically detect and segment non-degenerated or normal intervertebral discs from MR images and he used proton density (PD) weighted and T2 weighted sequences of MR images of the lumbar spine. Chevrefils et al. (Chevrefils et al., 2007) used the watershed technique along with some morphological operations for segmentation of the intervertebral discs. And he worked on thoracic spine images and medic modality. Shil et al. (Shi et al., 2007) worked on the detection of spinal cord using MR images of whole spine and for this task he employed Hough transform. After detection, he utilized methods of edge detection and self-adaptive window to locate and segment the discs. Finally, Wachter et al. (*(PDF) AUTOMATIC SEGMENTATION OF CERVICAL SOFT TISSUE FROM MR IMAGES*, n.d.) used T1 weighted and T2 weighted MR sequences of cervical spine and he used two methods; active shape models and fuzzy connectedness to get satisfactory results. But, none of these methods were employed to quantitatively evaluate the accuracy of segmentation results. Intensity based techniques have

12

proved insufficient for disc segmentation tasks as there occurs overlapping of the gray-scale values of the target tissue and the surrounding structures i.e. annulus fibrosus of disc has similar gray values as the anterior an posterior ligaments and nucleus pulposus has gray values similar to vertebral bodies. Moreover 2D images of spine have relatively low spatial and contrast resolution than 3D images and therefore, there occurs blurring over the disc boundaries and due to partial volume averaging (Pham et al., 2000). Since there still exists the possibility of user interaction errors in semi-automatic methods, therefore, to improve diagnostic efficiency and lessen the risk of inter-observer variability, semi-automatic and fully automatic methods may help in this regard. And many machine or deep learning based methods have been employed so far for this purpose discussed below.

2.1 Atlas Based Methods

Average description of spatial information of the anatomical images is termed as an anatomical atlas and this spatial information is used when segmentation by registration is considered as a method of choice (Rohlfing et al., 2005). For these methods, an atlas is constructed at first using rigid landmark-based image registration. Atlas based segmentation uses the training images that have been labeled previously to segment the region of interest in test images. Biasing from the background can occur in the resulting image which can be corrected in many ways. Probabilistic method resulted in better segmentation due to decrease in the border leakage error. FCM and extensions of FCM like Robust FCM methods have been used in combination with probabilistic atlas(Michopoulou et al., 2009).
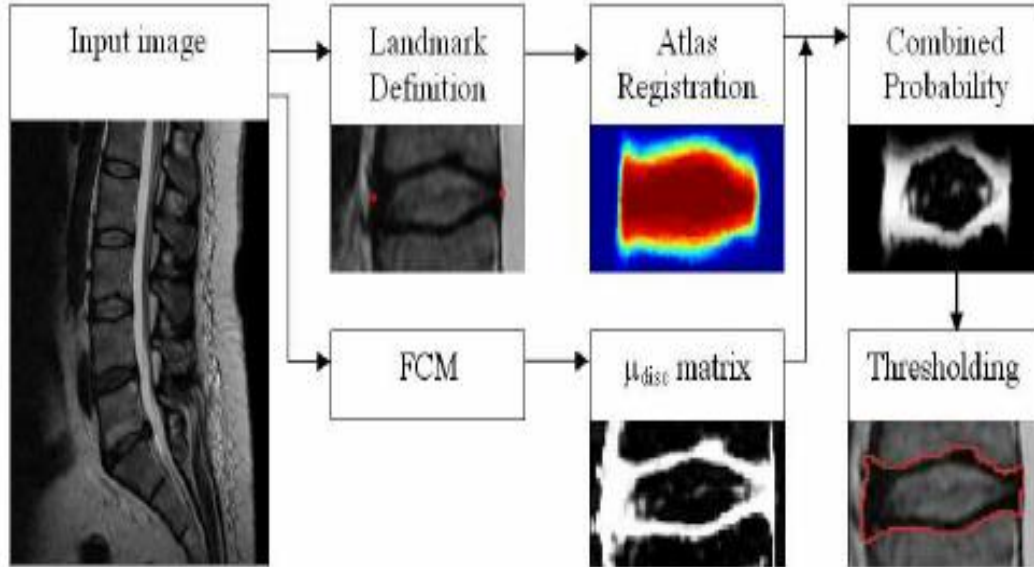
Figure 11 An Outline of Atlas-FCM Segmentation Method. Adapted from (Michopoulou et al., 2009)

2.2 FCM Algorithms

Fuzzy c means algorithms are soft techniques to remove partial volume averaging artifacts around the boundaries of region of interests like brain tumor or intervertebral discs. Extensions of FCM algorithms also exist like robust FCM (RFCM) and adaptive FCM which account for introducing smoothness and correcting for image intensity inhomogeneities deals with image noise (Michopoulou et al., 2009). Fuzzy clustering is different from K clustering as in K clustering one data point belongs to one cluster and in fuzzy algorithm each data point may belong to more than one the cluster. In case of IVD localization and segmentation tasks this algorithm uses an iterative process to find out the values of tissues class for every pixel of disc image. The resulting values basically represent the types of tissue (bone, disc, CSF) within a 3D pixel or voxel (Parveen et al., 2006) and thus can be used for segmenting images affected by an artifact of partial volume averaging (Pfirrmann et al., 2001). Fuzzy c means algorithms have also been used in combination with probabilistic anatomical atlas for better segmentation results. In this method (Michopoulou

14

et al., 2009), tissue class membership values are multiplied pixel by pixel with the atlas registered values of disc. And when interclass variance is minimized then combined probability matrix can be obtained automatically according to the method used by Otsu (Otsu, 1979). And in the end, a flood-fill operation can be used to fill empty spaces present in the disc and in the end resulting boundaries are smoothed by using morphological closing

2.3   CNN Free Mathematical Approach

Using morphological structure like tree of shapes and by some prior knowledge regarding target area and contrast differences in different modalities of MRI, target structures can be segmented correctly (Carlinet & Géraud, 2019). Both 2D and 3D images can be processed using such morphology. The tree of shapes is a powerful tool which can be used for many computer vision tasks including segmentation (Xu et al., 2016) and detailed information regarding images can be encoded into this structure to achieve better segmentation results and this is also used for pattern recognition tasks (Cao et al., 2008). Following are steps included in segmenting discs through this mathematical approach:

- Obtaining knowledge regarding IVDs localization

- Preparing a 3D volume

- Identification of discs in 2D images

- 3D regularization

Then the segmentation accuracy is measured using DICE metric which came out to be 0.816 with a lesser standard deviation statistics (Zheng et al., 2019). The main advantage of this method is its processing speed. And despite being learning free method, it is able to be compared with CNN approaches.
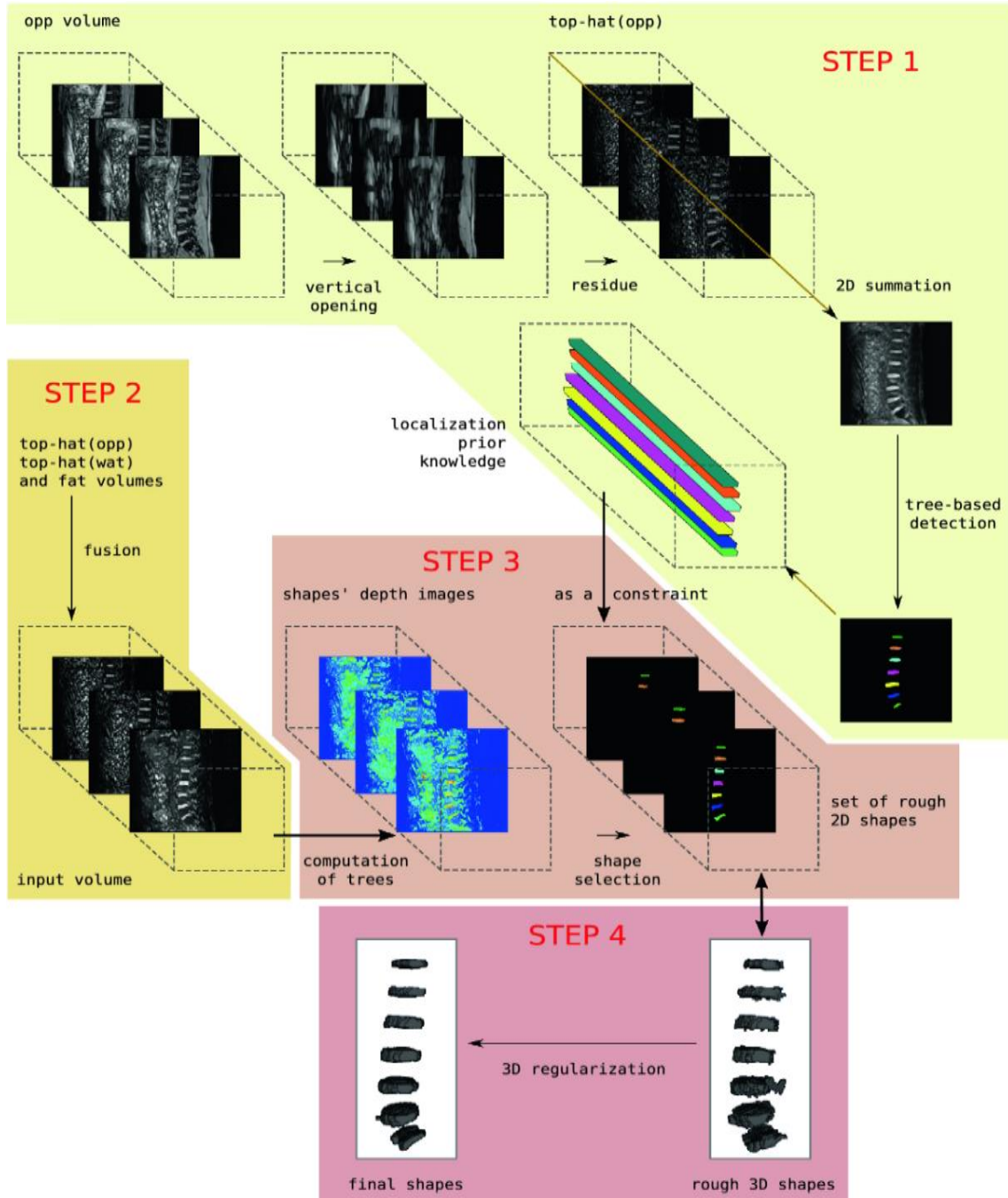
Figure 12 CNN-Free Mathematical Approach for IVD Segmentation. Adapted from Carlinet & Géraud, 2019

2.4 U-Net Segmentation

Convolutional neural networks (CNNs) have shown best results in localizing and segmenting medical images like brain tumors and IVDs (Chen et al., 2016), (Zheng et al., 2017), (Li et al., 2018). For example, Ji et al. (Ji et al., 2016) suggested such a standard convolutional neural network in which they used patch strategy i.e. they extracted patches around each pixel and hence performed the prediction and they used different patch dimensions like 2D and 2.5D for this IVD segmentation task. But the only drawback was that they worked on singe MRI modality. Using MR images of different sequences and incorporating them into deep learning segmentation networks has achieved attention recently. In convolutional neural networks, early and late fusion strategies have been addressed i.e. in early fusion strategy, low level features of the input images from all modalities or sequences are combined at the input level (Dolz et al., 2020),(Valverde et al., 2017) considering linear relationship between them whereas in late fusion strategy all sequences are processed with independent CNN and merged in deep layer. Although the segmentation result of late fusion strategy proves to be better than early fusion strategy [28], but still these strategies work in a single layer which cannot deal with the non-linearity and complex features of different sequences of MR images. In solution to this complexity, another Hyperdense Network has been used in which there are multiple connections which are not only confined to the layers of same path but also exist between layers across different paths (Nie et al., 2016). And they named network as U-Net model (Dolz et al., 2018) where one path is encoding (contracting) and the other is decoding (expanding). This method has also been used on multimodality MR images of Brain tumor localization and segmentation. And in IVD segmentation task, DSC for late fusion strategy came out to be 0.9086 which is lower than hyper-densely connected IVD-Net architecture whose DICE value is 0.9162.
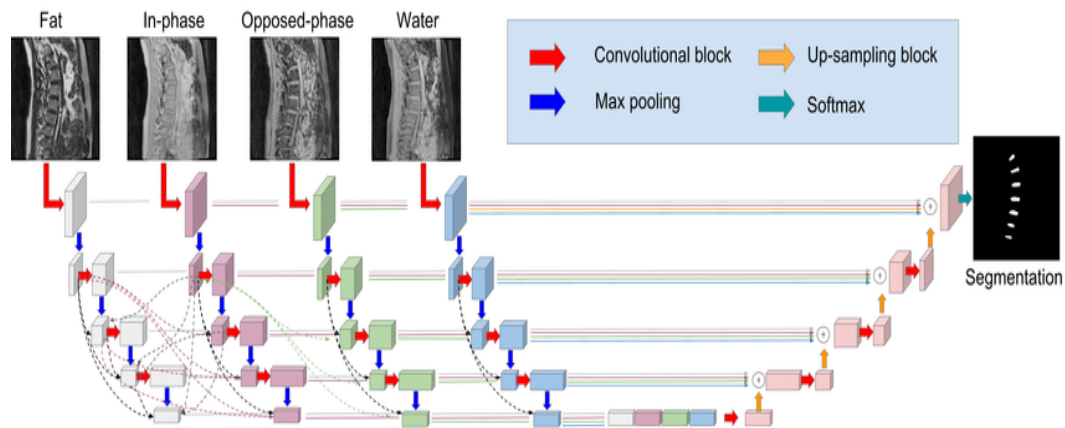
Figure 13 U-Net Model for IVD Segmentation. Adapted from (Dolz et al., 2018)

2.5   Segmentation Using V-Net

V-net is a 3D segmentation technique based on volumetric fully convolutional network (Iriondo & Girard, n.d.). It is similar to U-net but there exist some differences. IVD agonist V-net has been used to change the orientation of the sections around individual discs to a standard orientation for efficient segmentation. In this method, first key points are localized and labeled using random forests of FCNs and then CRFs are used to model the shape. These re-oriented IVDs are then sampled around each prediction. And then using FCN V-Net, IVDs are segmented. Back projection is used on the segmentation and relabeled according to the initial CRF labels. Finally, these segmentations are evaluated using DICE score. (*Review: V-Net — Volumetric Convolution (Biomedical Image Segmentation) | by Sik-Ho Tsang | Towards Data Science*, n.d.)

18
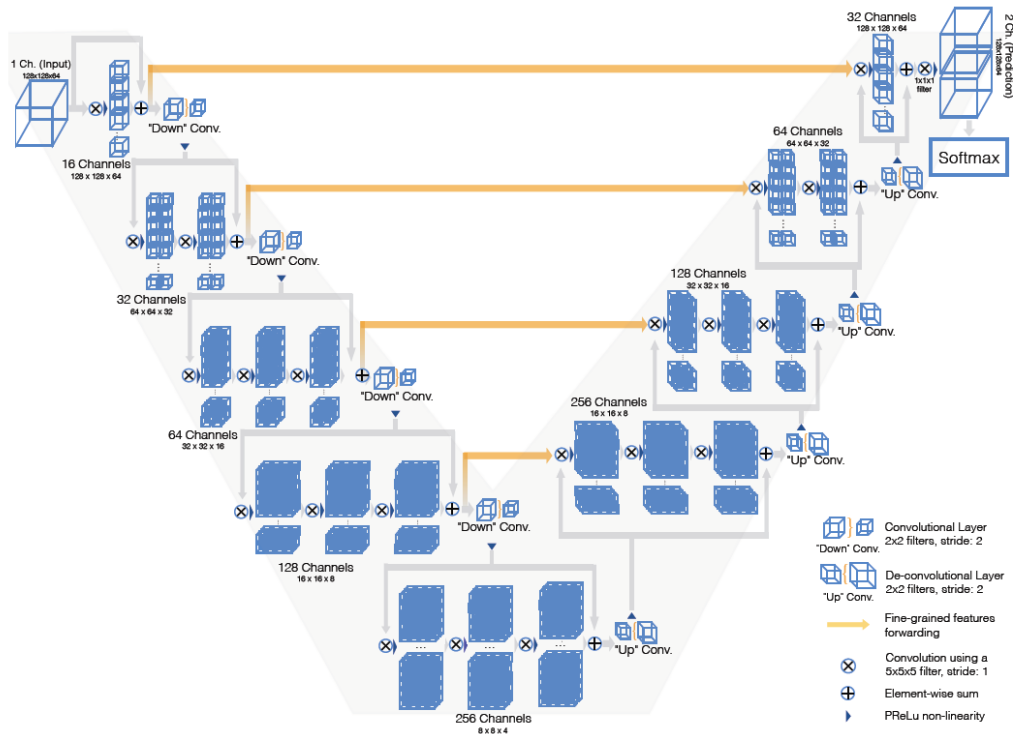
Figure 14 Schematic Representation of V-Net. Adapted from V-Net — Volumetric Convolution (Biomedical Image Segmentation) | by Sik-Ho Tsang | Towards Data Science, *n.d.)*

2.6   Non-Learning Based Bimodal CT/MRI Method

In this method complementary information is derived from both CT and MRI modalities and it requires minimum amount of intervention and is not learning based (Liaskos et al., 2020). Various image processing and analysis stages are included i.e.

1. Image Registration

2. Otsu-Based Thresholding

3. Chan-Vese Based Segmentation

The only human intervention included in this method is determining the vertebral body region of interests on both modalities manually. And 3D ROIs of both modalities are geometrically transformed to match each other. To extract the vertebral bodies from CT images, Otsu's thresholding-based method is used in which three labels are defined. Label 1 is for background and Labels 2 and 3 are for grey and white pixels and after further processing i.e. binary imaging, inter-slice correction and dilation vertebral boundaries are extracted. The extracted CT image is then projected onto the normalized MRI image and grey values are set to zero.

Intervertebral discs are then localized by considering the non-zero regions as IVDs and the Chan-Vese Contour model is applied. And in the end the vertebral regions extracted from CT images are superimposed on MR spinal images to separately define the vertebral bodies and intervertebral discs. DICE similarity coefficient and Hausdorff Distance have been used as evaluation metrics for this bimodal segmentation method and which were approximately 94% for CT and 86% for MRI and HD was 4.4 pixels for CT and 4.5 pixels for MRI. Given its efficiency, this method has proved comparable to the other state of the art learning-based methods.

3   CHAPTER 3: METHODOLOGY

3.1   Data Set

The dataset for this experiment was taken from IVDM3SEG challenge present at grand challenge.org. The data consists of MRI sequences of lower back containing at least 7 IVDs in every sequence. There is a total of 16 3D image sets from 8 subjects. Each subject was scanned under a 1.5-Tesla MRI scanner of Siemens using Dixon technique. Each image consists of 4 multi-modal MRI sequences of high resolution. The four modalities being fat, water, in phase, and out of phase. A binary mask corresponding to every image is also given. The spatial size of every sagittal slice is 512x512 pixels or 512x512x1 as these are only one channel images. The images include four volumes per subject and one binary volume per subject and these are stored in the Neuroimaging Informatics Technology Initiative (NIFTI) file format. There are actually 96 concatenated images in 16 3D volumes, hence there are 96 2D images in each modality.

96 x 16 x 4 = 6144 images in total.

96 x 13 = 1248 images for training of one modality

96 x 3 = 288 images for testing (one modality)

As in all previous works, researchers have divided the 16 3D volumes data into 13 volumes for training and 3 volumes for testing so I have also used the same division. In addition, I have also divided the train data into 80% train set and 20% validation set to avoid overfitting. Though there is no proper numeric for overfitting estimation but validation has been used so there is very little chance of overfitting. So results were checked in the first place for the validation set and then for the test set. So there is twofold validation of results.

3.2 Data Pre-Processing

The data provided at the challenge site consisted of 3D volumes of MRI scans in .nii format. These volumes were used to extract 2D sagittal slices. Each of these images was then subject to normalization. With this minimal pre-processing the images were used to train u-net. A slice of same image from different modalities and its corresponding mask is shown below.

The reason for choosing u-net over other networks is simple. According to Vuola *et al.* (Vuola et al., 2019), u-net performs better than the likes of Mask RCNN on medical datasets. 4 different u-nets were trained on the 4 different sequences.
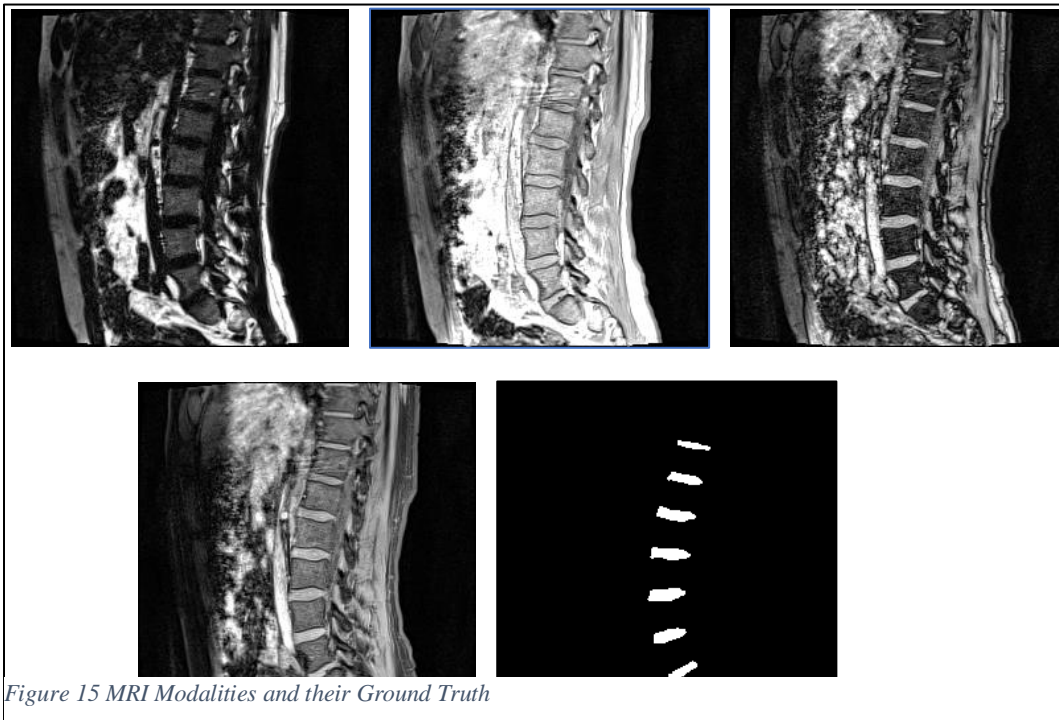
Figure 15 MRI Modalities and their Ground Truth

Figure 16 MRI Modalities and their Ground Truth

All the experiments were carried out in Google's Colab platform and I am thankful to them for providing free access to powerful GPUs. Moreover, I used Pytorch and FastAI to train models on my data.

3.3   Training U-Net for Different Modalities

We have treated this task as a semantic segmentation task since our goal is to only divide the pixels into IVD and non-IVD class and we do not care about what instance of IVD a particular pixel belongs to. That can be a task for some future study.

Now, instead of using the stock u-net, I chose to go with residual u-net. Residual u-net differs from the original in the fact that is has a resnet backbone in its contracting path and its reverse in the expanding. Thus, the conventional convolution blocks are replaced by more efficient residual blocks. A representation of residual u-net is given below:
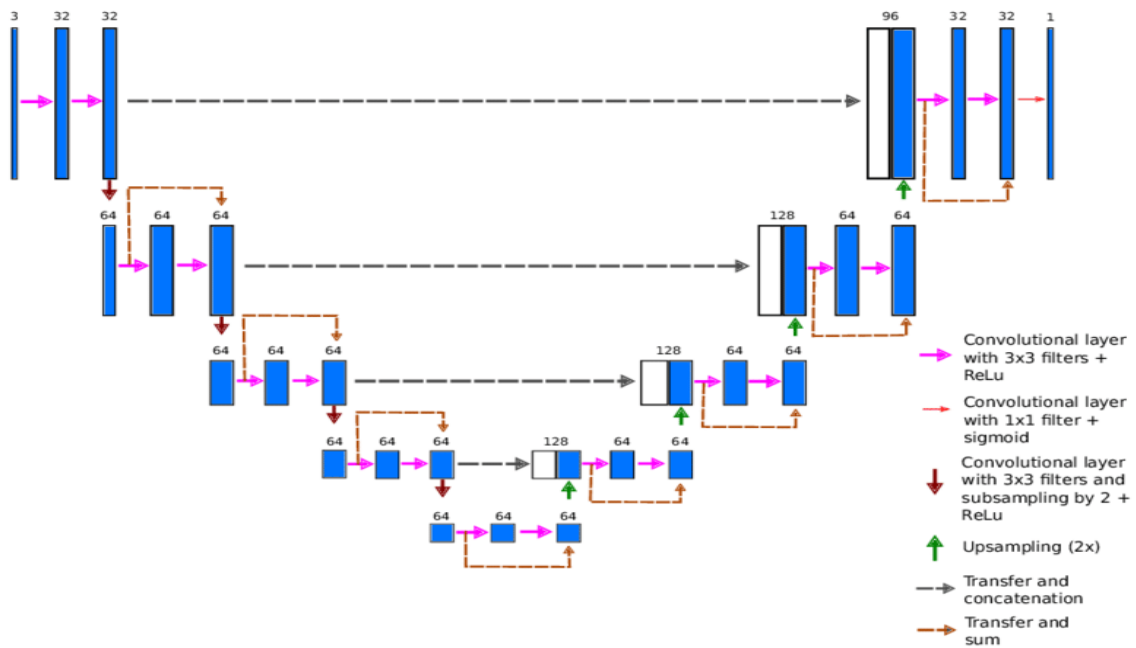
Figure 17 Representation of a Residual U-Net Model

23

For this particular case, Resnet34 backbone is chosen. The backbone is first trained on Imagenet dataset and then plugged into the u-net. The whole network is fine-tuned on given data. The data from every sequence is first divided into training, validation, and test sets. I used the 4 different modalities of the data to train 4 different u-nets, one for each modality. Each of these u-nets was trained for a total of 100 epochs. The hyper-parameters used for training the network are given below:

Hyper-parameters	Values
Epochs	100
Weight Decay	0.01
Base Learning Rate	0.0001
Min. Learning Rate (Layer specific Lr.)	0.0000025
Max. Learning Rate Period (Cyclic Lr.)	90% of the epoch
Optimizer	Adam Optimizer

Table 1 Hyper-parameters used for model training

For optimization of the weights of the filters, Adam Optimizer is used in training of the model which is basically an adaptive learning rate. In order to achieve faster convergence with lesser risk of getting stuck in local minima, I made use of the following techniques(Howard & Ruder, n.d.).

3.3.1 Cyclic Learning Rate

This technique is extracted from (Howard & Ruder, n.d.). The author states that in order to achieve better convergence on your data, a dynamic learning rate is better instead of static one. We have learning rate scheduled for that, but the author has argued upon changing the learning rate within the same epoch. A cyclic learning rate first increases linearly from the base learning rate to a maximum value for a given percentage of iterations and then linearly falls back to its original value

for the rest of the epoch and the process continues for the next epochs. It is better understood by the diagram below:
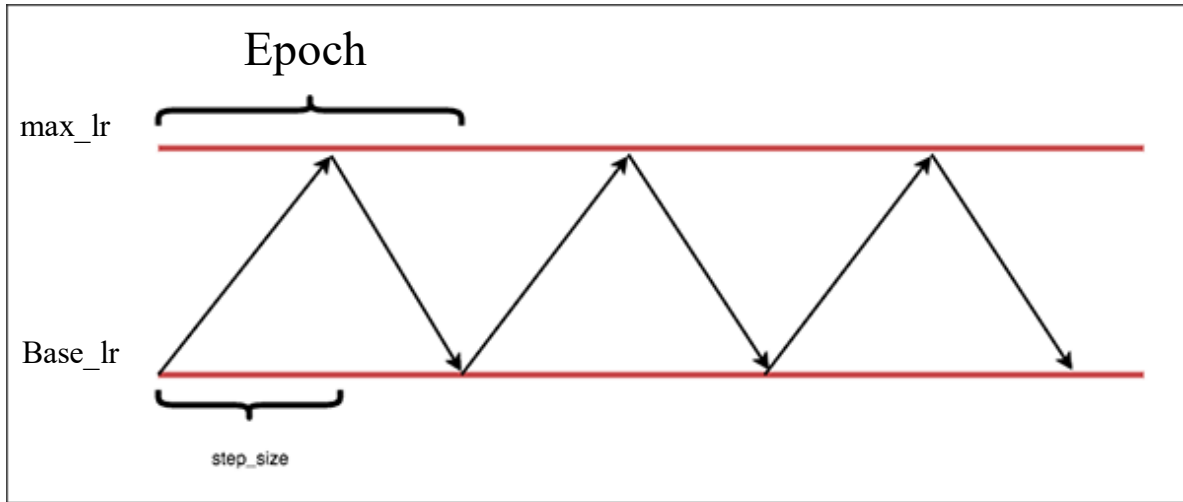
Figure 18 Diagrammatic Representation of Cyclic Learning Rate

In this study, I chose step size as 90% of the epoch.

3.3.2 Layer-specifics Learning Rate

According to the authors of (Howard & Ruder, n.d.), all layers in a network do not require the same learning rate. The first layers of the network extract raw and crude features from the data whereas as you move deeper into the layers, the features extracted by the layers become more and more sophisticated. For example, the first few layers of a face detector might only detect lines, texture, color, etc. features that are common throughout different datasets. On the other hand, the last layers detect more data-specific features like maybe nose, eyes, mouth etc.

So, we do not need to treat every layer with the same learning rate. In order to attain a better convergence, it is better to use different learning rates for different layers. The first ones get the least learning rate while the last ones get the highest. In my case, the layers were divided into 3 different groups and every group was assigned a different learning rate. The group of layers closer to the input had a learning rate of 2.5e-7 while the middle group had 1.2625e-5 while the last group of layers had a learning rate of 2.5e-5.

First Layer   Middle Layer   Final Layer

lr=2.5e-7   lr=1.2625e-5   lr=2.5e-5
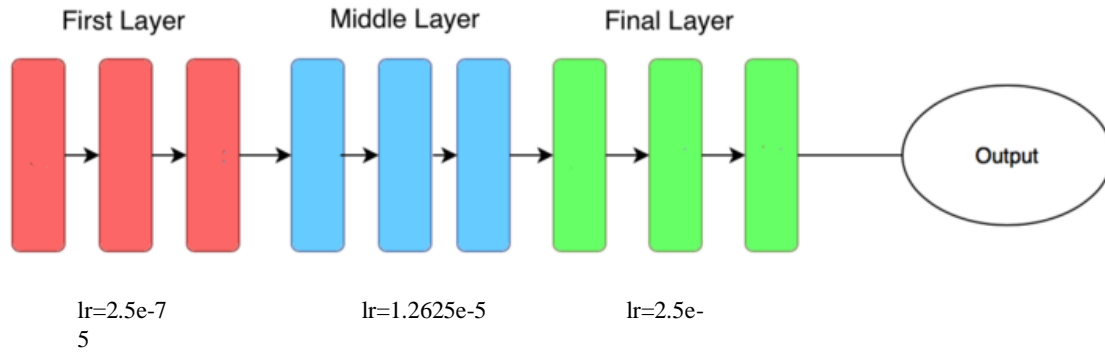
Figure 19 Learning Rate in Different Layers.

The 4 u-net trained on the 4 modalities could be used as standalone models for segmentation of IVDs, but I decided to take it up a notch and make something on top of it. The architecture of the U-Net model proposed in this study is:
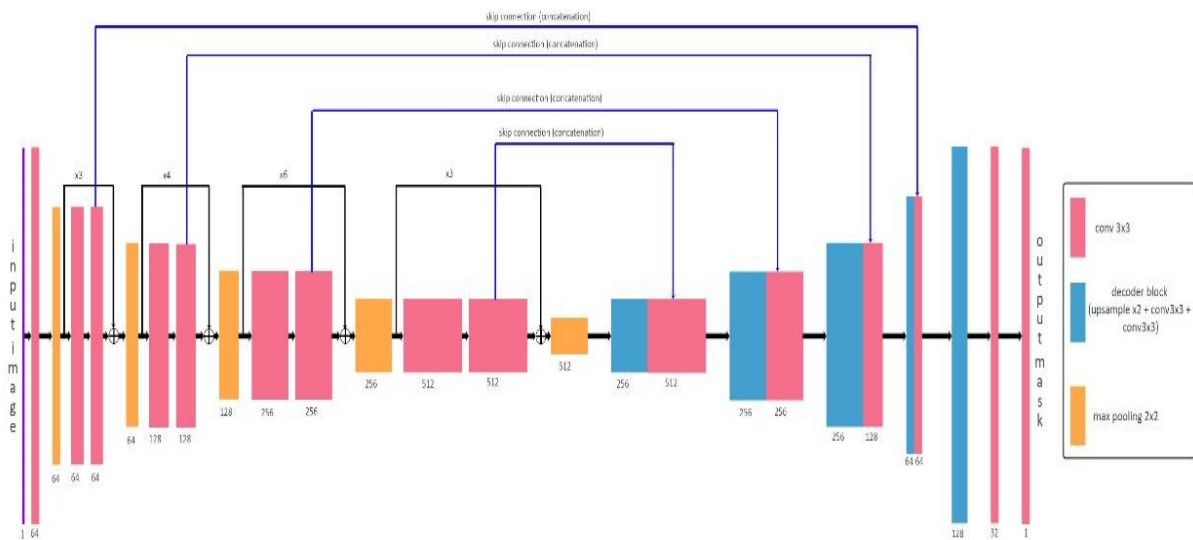
Figure 20 Proposed U-Net Architecture

3.4 Ensemble Creation with U-nets

With the 4 networks trained, I created an ensemble model of the 4 to leverage the power of data as much as I could. For this purpose, I chose to go with stacked ensemble. A u-net was further trained

on the outputs of the 4 models in the previous section. The hyper-parameters used for this ensemble model training are same as used earlier for initial modality trainings except for the number for epochs. The outputs were concatenated with each other and the ensemble model was trained on that as the input. Cyclic learning rate and layer specific learning rate were again used and this time the network was trained for 40 epochs.

It is better understood with the diagram below:
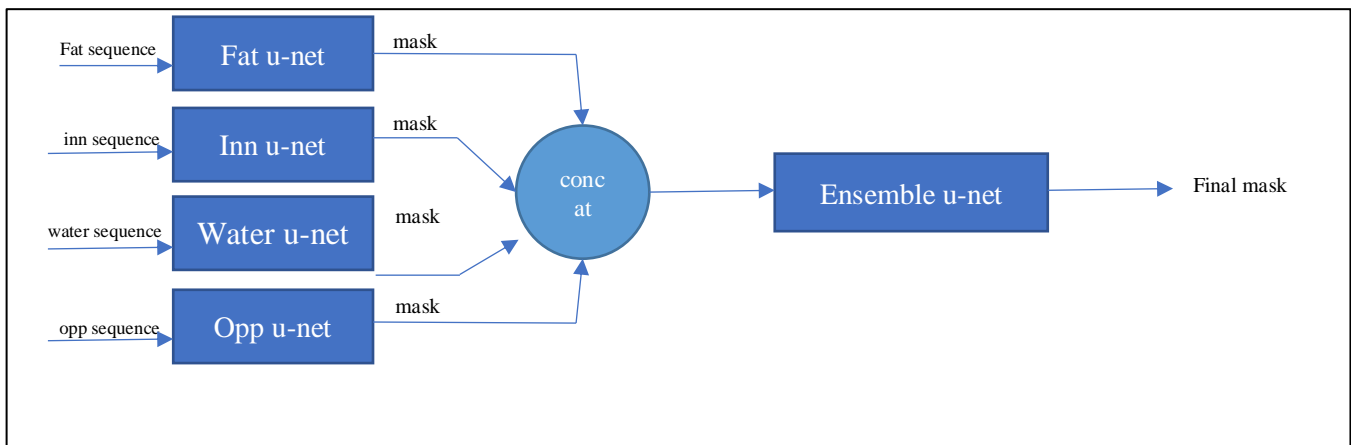
Figure 21 Diagrammatic Representation of U-Net Model Training with Ensemble Model.
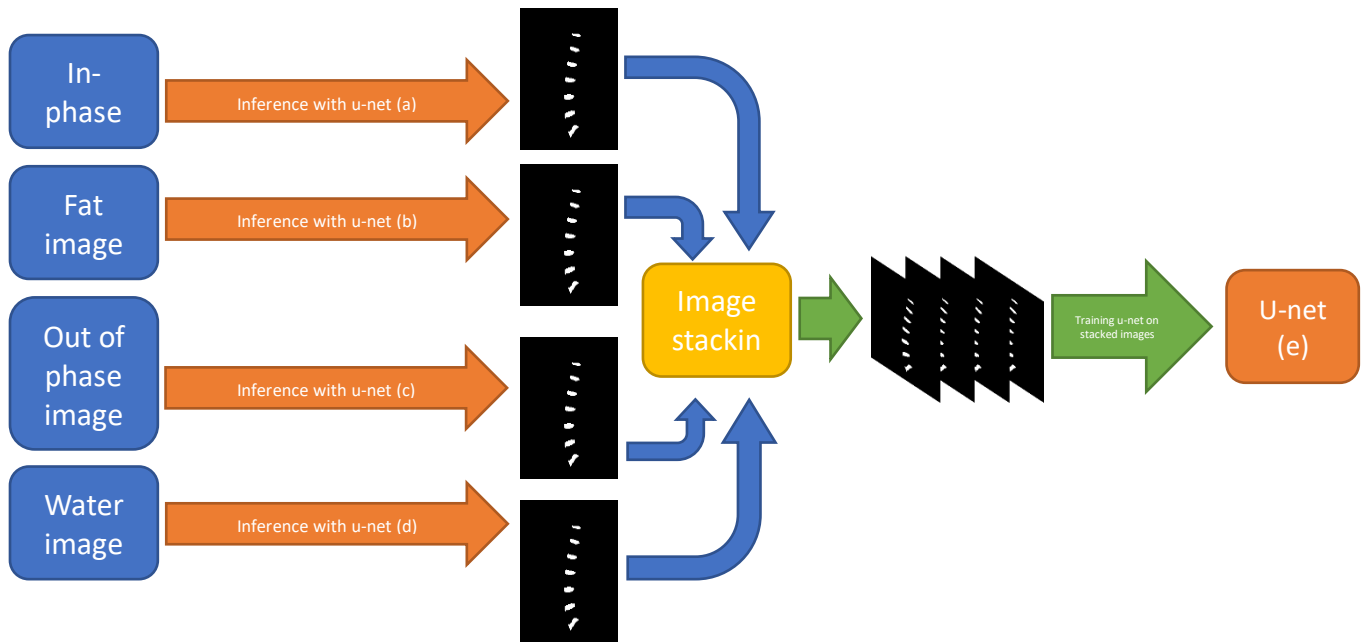
Figure 22 Ensemble model with mask images

27
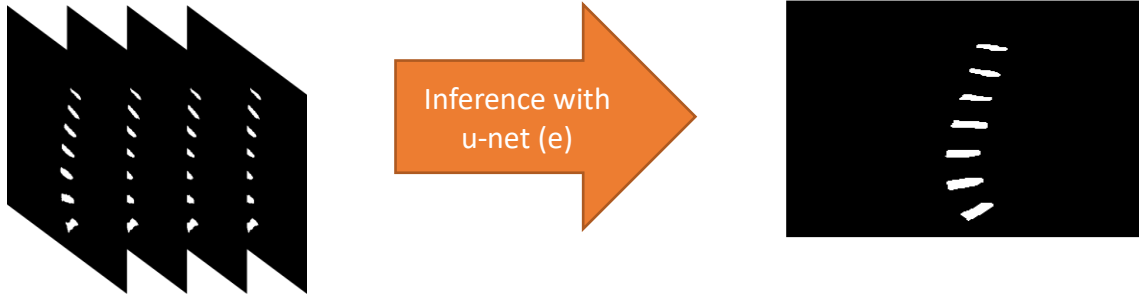
Figure 23 Final mask output

3.5 Evaluation Metrics

Intermediate and final models were evaluated based on Dice Score (DSC), Mean Surface Distance (MSD), and Hausdorff Distance (HD) metrics.

3.5.1 Dice Score

Dice score or dice coefficient of segmentation can be considered as the pixel level F1 score. Mathematically, it is represented as

$$DSC = 2 * \frac{|GT \cap Pred|}{|GT| + |Pred|}$$

Where,

GT is the ground truth mask,

Pred is the predicted mask,

$\cap$ represents intersection, and
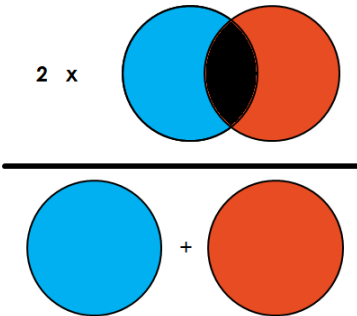
|| is the cardinality or the number of elements

If we think of pixels in terms of true positives (TP), false positives (FP) and false negatives (FN), DSC can be written as

$$DSC = \frac{2TP}{2TP + FP + FN}$$

28

As can be seen from the above equation that it is indeed the F1 score for segmentation.

$$DSC =$$

3.5.2 Surface Distance

Surface distance is the measure of the distance between a point (pixel) on one surface and a corresponding point on another surface. In our case, we calculated the surface distance between the given labels and the inference masks. Euclidean distances between all the surface pixels in the labels and the closest point on the prediction are calculated. Surface distance itself might not be a very good indicator of the segmentation so I calculated the following two derivatives of surface distance.

3.5.3 Mean Surface Distance

As the name suggests, it is, simply, the mean of the surface distances of all the surface points. It measures how much does the prediction digress from the ground truth on average.

3.5.4 Hausdorff Distance

Hausdorff distance is the maximum distance between a pixel in the given label and a corresponding pixel in the prediction. In simple words, given that we have found the surface distances of all the surface pixels for a given image, Hausdorff distance is the maximum value of all those distances. Hausdorff distance can be a good metric since it measures the maximum range that the prediction differs from the ground truth.

4 CHAPTER 4: RESULTS

4.1 Evaluation of intermediate and final models

Once the intermediate models were trained, I evaluated them of the test set and after training the final ensemble model, I evaluated the predictions again. Note that the values of MSD and HD are in pixels. These results are summarized in the table below.

	Fat	In phase	Out of phase	water
MSD	0.1060	0.1395	0.2208	0.1875
HD	1.0120	1.0420	1.3805	1.2596
Dice	0.9754	0.9673	0.9468	0.9558

Table 2 Result of Intermediate Models

After the creation of ensemble model, the evaluation results came out as follows.

	Ensemble model
MSD	0.0383
HD	0.9855
Dice	0.9910

Table 3 Result of Ensemble Model

As can be inferred from the results that the model performs excellently. Let us visualize predictions from different models on the same image in different modalities.
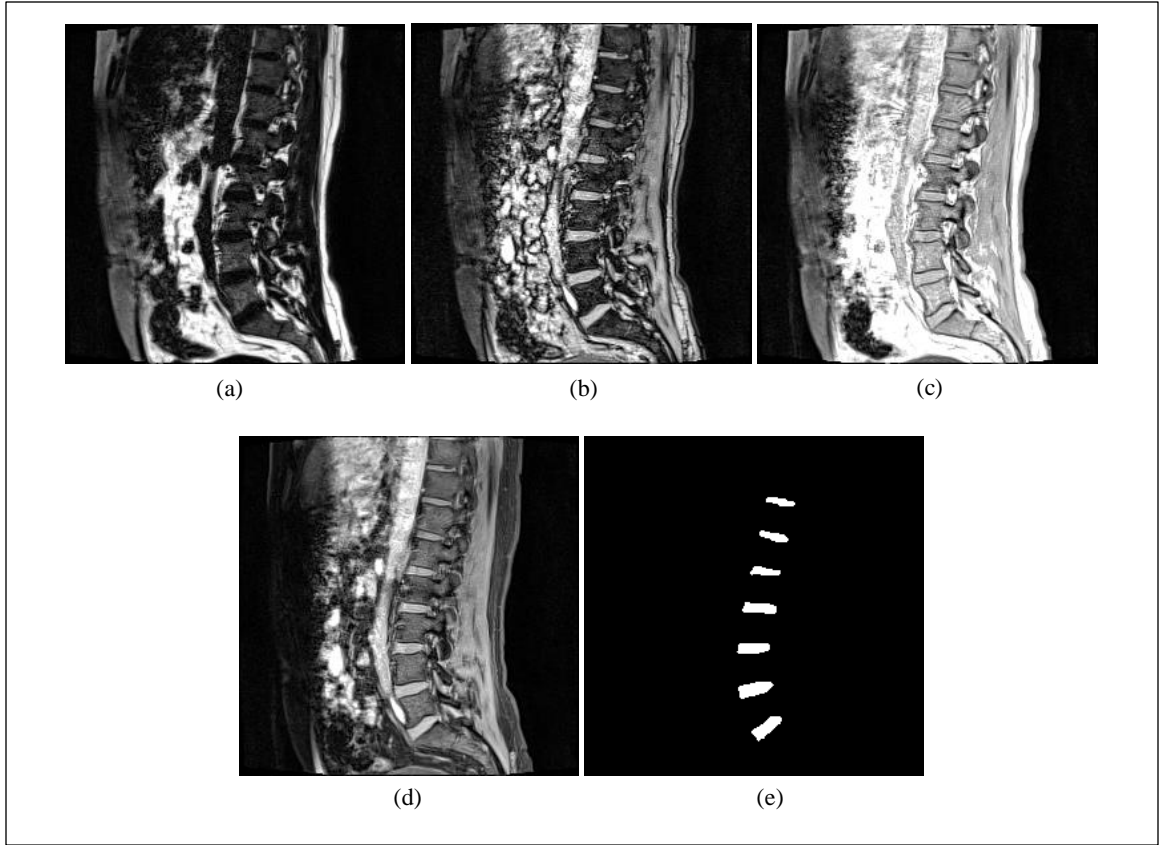
Figure 24 Input images. (a) fat, (b) out of phase, (c) in phase, (d) water, (e) ground truth label

Naked eye can barely make the difference between the prediction of ensemble model and the ground truth label. The percentile statistics of the prediction masks are shown in the following table:

MODALITIES	DICE	MSD	HD
FAT	**75th percentile:** 0.9744876620660812 **50th percentile:** 0.9748850371418465 **25th percentile:** 0.9693593314763231	**75th percentile:** 0.12247071352502663 **50th percentile:** 0.12572533849129594 **25th percentile:** 0.10597302504816955	**75th percentile:** 1.0 **50th percentile:** 1.0 **25th percentile:** 1.0
WATER	**75th percentile:** 0.9576988155668359 **50th percentile:** 0.9653954802259888 **25th percentile:** 0.9483227561196736	**75th percentile:** 0.20042643923240938 **50th percentile:** 0.1803794163256719 **25th percentile:** 0.17346150581095462	**75th percentile:** 1.0 **50th percentile:** 1.4142135623730951 **25th percentile:** 1.4142135623730951
IN PHASE	**75th percentile:** 0.9635220125786164 **50th percentile:** 0.9689265536723164 **25th percentile:** 0.9633699633699634	**75th percentile:** 0.17057569296375266 **50th percentile:** 0.16247582205029013 **25th percentile:** 0.12761904761904763	**75th percentile:** 1.0 **50th percentile:** 1.0 **25th percentile:** 1.0
OUT OF PHASE	**75th percentile:** 0.9561551433389545 **50th percentile:** 0.9662522202486679 **25th percentile:** 0.9314553990610329	**75th percentile:** 0.2132904608788853 **50th percentile:** 0.17201166180758018 **25th percentile:** 0.23736435084877533	**75th percentile:** 1.0 **50th percentile:** 1.0 **25th percentile:** 1.4142135623730951

Table 4 Evaluation Statistics of all modalities and ensemble

5   CHAPTER 5: DISCUSSION

In this study, a new version of U-Net model is proposed for better segmentation results in which residual blocks are used in place of conventional convolutional blocks like the ones used in (Dolz et al., 2020). In this proposed method first of all four different modalities of MR imaging are used for better precision of intervertebral discs. These images from different sequences are then fed into four different U-Net models and then output models are stacked over each other to formulate an ensemble model which has refined the outputs of all sequences and thus giving the state of the art results as compared to the previously used methods. The novelty introduced into this model training is the use of fastest convergence techniques which are cyclic learning rate and layers specific learning rate. The U-Net model or IVD-Net model that is used in (Dolz et al., 2018) used the concept of inception modules and also compared with early and late fusion strategies. But using techniques of using residual blocks with concatenation of output with inputs and employing the techniques of cyclic and different learning rates for every layer has improved the segmentation results markedly.   The comparison between the results of previously used techniques and this proposed network is given below:

Architecture	DSC	Localization distance (voxels)
Baseline EarlyFusion	0.8981 ± 0.0293	0.7701 ± 1.5872
Baseline LateFusion	0.9086 ± 0.0339	0.7400 ± 1.6009
IVD-Net	0.9162 ± 0.0192	0.4145 ± 0.2698
IVD-Net (asym)	0.9191 ± 0.0179	0.4470 ± 0.2641
2D U-Net Model with Ensemble U-Net Network	**0.9910**	MSD=0.0383 HD=0.9855

Table 5 Comparison of Four Different Segmentation Techniques. Adapted from (Dolz et al., 2018)

So far many techniques including U-Net have been used for intervertebral discs segmentation like probabilistic atlas based fuzzy c-means method or fusion strategies in hyper dense network but none of them gave the dice score above 92%. The ensemble of four U-net models and hyper parameters used in this study have given the dice score of 99%. Moreover, there is another

technique of mask RCNN which is considered to be the best segmentation technique but according to Vuola, this method gives the good segmentation results in non-medical objects (Vuola et al., 2019). For anatomical structures, U-Net model training is so far superior to other techniques and more improvements can be made in it to further improve the results.

6   CHAPTER 6: CONCLUSION

This study focuses on a medical task of intervertebral disc segmentation from given MR images of different sequences or modalities. The purpose of this study is to accurately segment the intervertebral discs that can aid neurosurgeons for spinal surgeries. This is done via a supervised deep learning technique which is a U-Net architecture that can efficiently leverage information from multiple MRI sequences, all in sagittal plane, for IVD segmentation. Following recent research on intervertebral discs segmentation, my architecture not only adopts dense connections between multiple paths but also adopts different fastest convergence techniques like cyclic learning rate and layer-specifics learning rate and for better results, outputs of all individually trained U-Nets for separate modalities are then ensembled on top of each other. It is demonstrated that previously used techniques like fusion strategies and mask RCNN are not sufficient to fully use the information in different MRI sequences. When the network learns the features from different sequences, it better understands the complex relationships between multiple sources. Which helps in improvement of its representation power and ultimately better output is obtained.

7   CHAPTER 7: FUTURE WORK

This task is treated as semantic segmentation where pixels are only classified as IVD pixels and non-IVD pixels. In future work the idea of knowing about what instance of IVD a particular pixel belongs to can be another task. Moreover there are many other MRI modalities which are used to diagnose intervertebral disc changes other than four given in the data set. So, Model can be trained on other modalities as well for better accuracy of results. This model is trained to segment the normal discs Another task which can be included in future studies for further improvement in segmentation accuracy can be the use of three planes for segmentation rather than one plane which are sagittal, axial and coronal sections. That would be more helpful while localizing the degenerative discs in place of normal ones. Because the degeneration can be of different types including disc bulges, disc emaciation, disc herniation and osteophyte formation. Also the disc shape, disc location and extent of degeneration may vary from patient to patient and that would be a limiting factor or a huge load of data may be required to train the model for segmentation of such worn out discs. In further studies both MRI and CT scan modalities can be combined for more efficient segmentation of both vertebral bodies and intervertebral discs as both modalities provide separate feature information regarding bone and discs.

8 Bibliography

(PDF) AUTOMATIC SEGMENTATION OF CERVICAL SOFT TISSUE FROM MR IMAGES. (n.d.). Retrieved May 11, 2021, from https://www.researchgate.net/publication/237558371_AUTOMATIC_SEGMENTATION_ OF_CERVICAL_SOFT_TISSUE_FROM_MR_IMAGES

Adams, M. A., & Roughley, P. J. (2006). What is intervertebral disc degeneration, and what causes it? In *Spine* (Vol. 31, Issue 18, pp. 2151–2161). Spine (Phila Pa 1976). https://doi.org/10.1097/01.brs.0000231761.73859.2c

An, H. S., Anderson, P. A., Haughton, V. M., Iatridis, J. C., Kang, J. D., Lotz, J. C., Natarajan, R. N., Oegema, T. R., Roughley, P., Setton, L. A., Urban, J. P., Videman, T., Andersson, G. B. J., & Weinstein, J. N. (2004). Introduction. Disc degeneration: Summary. In *Spine* (Vol. 29, Issue 23, pp. 2677–2678). Spine (Phila Pa 1976). https://doi.org/10.1097/01.brs.0000147573.88916.c6

Broadhouse, K. M. (2019). The Physics of MRI and How We Use It to Reveal the Mysteries of the Mind. *Frontiers for Young Minds*, *7*. https://doi.org/10.3389/frym.2019.00023

Can Stem Cells Help Reverse Degenerative Disc Disease? (n.d.). Retrieved May 11, 2021, from https://stemcellthailand.org/therapies/degenerative-disc-disease-ddd/

Cao, F., Lisani, J. L., Morel, J. M., Musé, P., & Sur, F. (2008). A theory of shape identification. *Lecture Notes in Mathematics*, *1948*, 1–268. https://doi.org/10.1007/978-3-540-68481-7

Carlinet, E., & Géraud, T. (2019). Intervertebral disc segmentation using mathematical morphology—A CNN-free approach. *Lecture Notes in Computer Science (Including Subseries Lecture Notes in Artificial Intelligence and Lecture Notes in Bioinformatics)*, *11397 LNCS*, 105–118. https://doi.org/10.1007/978-3-030-13736-6_9

Chaturvedi, A., Klionsky, N. B., Nadarajah, U., Chaturvedi, A., & Meyers, S. P. (2018). Malformed vertebrae: a clinical and imaging review. In *Insights into Imaging* (Vol. 9, Issue 3, pp. 343–355). Springer Verlag. https://doi.org/10.1007/s13244-018-0598-1

Chen, H., Dou, Q., Wang, X., Qin, J., Cheng, J. C. Y., & Heng, P. A. (2016). 3D fully convolutional networks for intervertebral disc localization and segmentation. *Lecture Notes in Computer Science (Including Subseries Lecture Notes in Artificial Intelligence and Lecture Notes in Bioinformatics)*, *9805 LNCS*, 375–382. https://doi.org/10.1007/978-3-319-43775-0_34

Chevrefils, C., Chériet, F., Grimard, G., & Aubin, C. E. (2007). Watershed segmentation of intervertebral disk and spinal canal from MRI images. *Lecture Notes in Computer Science (Including Subseries Lecture Notes in Artificial Intelligence and Lecture Notes in Bioinformatics)*, *4633 LNCS*, 1017–1027. https://doi.org/10.1007/978-3-540-74260-9_90

Dolz, J., Desrosiers, C., & Ayed, I. Ben. (2018). IVD-Net: Intervertebral disc localization and segmentation in MRI with a multi-modal UNet. *Lecture Notes in Computer Science (Including Subseries Lecture Notes in Artificial Intelligence and Lecture Notes in Bioinformatics)*, *11397 LNCS*, 130–143. http://arxiv.org/abs/1811.08305

Dolz, J., Desrosiers, C., Wang, L., Yuan, J., Shen, D., & Ben Ayed, I. (2020). Deep CNN ensembles and suggestive annotations for infant brain MRI segmentation. *Computerized Medical Imaging and Graphics*, *79*, 101660. https://doi.org/10.1016/j.compmedimag.2019.101660

Frost, B. A., Camarero-Espinosa, S., & Johan Foster, E. (2019). Materials for the spine: Anatomy,

problems, and solutions. In *Materials* (Vol. 12, Issue 2, p. 253). MDPI AG. https://doi.org/10.3390/ma12020253

Guerini, H., Omoumi, P., Guichoux, F., Vuillemin, V., Morvan, G., Zins, M., Thevenin, F., & Drape, J. L. (2015). Fat Suppression with Dixon Techniques in Musculoskeletal Magnetic Resonance Imaging: A Pictorial Review. In *Seminars in Musculoskeletal Radiology* (Vol. 19, Issue 4, pp. 335–347). Thieme Medical Publishers, Inc. https://doi.org/10.1055/s-0035-1565913

Hamamci, A., Kucuk, N., Karaman, K., Engin, K., & Unal, G. (2012). Tumor-cut: Segmentation of brain tumors on contrast enhanced mr images for radiosurgery applications. *IEEE Transactions on Medical Imaging*, *31*(3), 790–804. https://doi.org/10.1109/TMI.2011.2181857

Howard, J., & Ruder, S. (n.d.). *Universal Language Model Fine-tuning for Text Classification*. Retrieved May 12, 2021, from http://nlp.fast.ai/ulmfit.

Hwang, D., Kim, S., Abeydeera, N. A., Statum, S., Masuda, K., Chung, C. B., Siriwanarangsun, P., & Bae, W. C. (2016). Quantitative magnetic resonance imaging of the lumbar intervertebral discs. In *Quantitative Imaging in Medicine and Surgery* (Vol. 6, Issue 6, pp. 744–755). AME Publishing Company. https://doi.org/10.21037/qims.2016.12.09

Iriondo, C., & Girard, M. (n.d.). *Vesalius: VNet-based fully automatic segmentation of intervertebral discs in multimodality MR images*. Retrieved May 11, 2021, from https://arxiv.org/abs/1606.04797

Ji, X., Zheng, G., Belavy, D., & Ni, D. (2016). Automated intervertebral disc segmentation using deep convolutional neural networks. *Lecture Notes in Computer Science (Including Subseries Lecture Notes in Artificial Intelligence and Lecture Notes in Bioinformatics)*, *10182 LNCS*, 38–48. https://doi.org/10.1007/978-3-319-55050-3_4

Li, X., Dou, Q., Chen, H., Fu, C. W., Qi, X., Belavý, D. L., Armbrecht, G., Felsenberg, D., Zheng, G., & Heng, P. A. (2018). 3D multi-scale FCN with random modality voxel dropout learning for Intervertebral Disc Localization and Segmentation from Multi-modality MR Images. *Medical Image Analysis*, *45*, 41–54. https://doi.org/10.1016/j.media.2018.01.004

Liaskos, M., Savelonas, M. A., Asvestas, P. A., Lykissas, M. G., & Matsopoulos, G. K. (2020). Bimodal CT/MRI-based segmentation method for intervertebral disc boundary extraction. *Information (Switzerland)*, *11*(9). https://doi.org/10.3390/INFO11090448

Michopoulou, S. K., Costaridou, L., Panagiotopoulos, E., Speller, R., Panayiotakis, G., & Todd-Pokropek, A. (2009). Atlas-based segmentation of degenerated lumbar intervertebral discs from MR images of the spine. *IEEE Transactions on Biomedical Engineering*, *56*(9), 2225–2231. https://doi.org/10.1109/TBME.2009.2019765

Modic, M. T., & Ross, J. S. (2007). Lumbar degenerative disk disease. In *Radiology* (Vol. 245, Issue 1, pp. 43–61). Radiology. https://doi.org/10.1148/radiol.2451051706

Nie, D., Wang, L., Gao, Y., & Sken, D. (2016). Fully convolutional networks for multi-modality isointense infant brain image segmentation. *Proceedings - International Symposium on Biomedical Imaging*, *2016-June*, 1342–1345. https://doi.org/10.1109/ISBI.2016.7493515

Niemeläinen, R., Videman, T., Dhillon, S. S., & Battié, M. C. (2008). Quantitative measurement of intervertebral disc signal using MRI. *Clinical Radiology*, *63*(3), 252–255. https://doi.org/10.1016/j.crad.2007.08.012

Otsu, N. (1979). THRESHOLD SELECTION METHOD FROM GRAY-LEVEL HISTOGRAMS. *IEEE Trans Syst Man Cybern*, *SMC-9*(1), 62–66. https://doi.org/10.1109/tsmc.1979.4310076

Parveen, R., Ruff, C., & Todd-Pokropek, A. (2006). Three dimensional tissue classifications in MR brain images. *Lecture Notes in Computer Science (Including Subseries Lecture Notes in Artificial Intelligence and Lecture Notes in Bioinformatics)*, *4241 LNCS*, 236–247. https://doi.org/10.1007/11889762_21

Pfirrmann, C. W. A., Metzdorf, A., Zanetti, M., Hodler, J., & Boos, N. (2001). Magnetic resonance classification of lumbar intervertebral disc degeneration. *Spine*, *26*(17), 1873–1878. https://doi.org/10.1097/00007632-200109010-00011

Pham, D. L., Xu, C., & Prince, J. L. (2000). Current methods in medical image segmentation. *Annual Review of Biomedical Engineering*, *2*(2000), 315–337. https://doi.org/10.1146/annurev.bioeng.2.1.315

Pooley, R. A. (2005). Fundamental physics of MR imaging. *Radiographics*, *25*(4), 1087–1099. https://doi.org/10.1148/rg.254055027

Review: V-Net — Volumetric Convolution (Biomedical Image Segmentation) | by Sik-Ho Tsang | Towards Data Science. (n.d.). Retrieved May 11, 2021, from https://towardsdatascience.com/review-v-net-volumetric-convolution-biomedical-image-segmentation-aa15dbaea974

Roberts, N., Gratin, C., & Whitehouse, G. H. (1997). MRI analysis of lumbar intervertebral disc height in young and older populations. *Journal of Magnetic Resonance Imaging*, *7*(5), 880–886. https://doi.org/10.1002/jmri.1880070517

Rohlfing, T., Brandt, R., Menzel, R., Russakoff, D. B., & Maurer, C. R. (2005). Quo Vadis, Atlas-Based Segmentation? In *Handbook of Biomedical Image Analysis* (pp. 435–486). Springer US. https://doi.org/10.1007/0-306-48608-3_11

Ruiz Wills, C. E. (2015). *A COMPUTATIONAL STUDY OF INTERVERTEBRAL DISC DEGENERATION IN RELATION TO CHANGES IN REGIONAL TISSUE COMPOSITION AND DISC NUTRITION*.

Schematic representation of magnetic resonance imaging principles. (A)... | Download Scientific Diagram. (n.d.). Retrieved May 11, 2021, from https://www.researchgate.net/figure/Schematic-representation-of-magnetic-resonance-imaging-principles-A-When-placed-in-a_fig1_334004270

Shi, R., Sun, D., Qiu, Z., & Weiss, K. L. (2007). An efficient method for segmentation of MRI spine images. *2007 IEEE/ICME International Conference on Complex Medical Engineering, CME 2007*, 713–717. https://doi.org/10.1109/ICCME.2007.4381830

The proper terminology for reporting lumbar intervertebral disk disorders - PubMed. (n.d.). Retrieved May 11, 2021, from https://pubmed.ncbi.nlm.nih.gov/9403442/

Tsai, M. D., Jou, S. Bin, & Hsieh, M. S. (2002). A new method for lumbar herniated inter-vertebral disc diagnosis based on image analysis of transverse sections. *Computerized Medical Imaging and Graphics*, *26*(6), 369–380. https://doi.org/10.1016/S0895-6111(02)00033-2

Valverde, S., Cabezas, M., Roura, E., González-Villà, S., Pareto, D., Vilanova, J.-C., Ramió-Torrentà, Ll., Rovira, À., Oliver, A., & Lladó, X. (2017). Improving automated multiple sclerosis lesion segmentation with a cascaded 3D convolutional neural network approach. *NeuroImage*, *155*, 159–168. http://arxiv.org/abs/1702.04869

van Vucht, N., Santiago, R., Lottmann, B., Pressney, I., Harder, D., Sheikh, A., & Saifuddin, A. (2019). The Dixon technique for MRI of the bone marrow. In *Skeletal Radiology* (Vol. 48, Issue 12, pp. 1861–1874). Springer Verlag. https://doi.org/10.1007/s00256-019-03271-4

Violas, P., Estivalezes, E., Briot, J., Sales de Gauzy, J., & Swider, P. (2007). Objective quantification of intervertebral disc volume properties using MRI in idiopathic scoliosis

surgery. *Magnetic Resonance Imaging*, *25*(3), 386–391. https://doi.org/10.1016/j.mri.2006.09.007

Vuola, A. O., Akram, S. U., & Kannala, J. (2019). Mask-RCNN and U-net Ensembled for Nuclei Segmentation. *Proceedings - International Symposium on Biomedical Imaging*, *2019-April*, 208–212. http://arxiv.org/abs/1901.10170

What Is Degenerative Disc Disease? - Orthopedic & Sports Medicine. (n.d.). Retrieved May 11, 2021, from https://orthosportsmed.com/what-is-degenerative-disc-disease/

Xu, Y., Géraud, T., & Najman, L. (2016). Connected Filtering on Tree-Based Shape-Spaces. *IEEE Transactions on Pattern Analysis and Machine Intelligence*, *38*(6), 1126–1140. https://doi.org/10.1109/TPAMI.2015.2441070

Zheng, G., Belavy, D., Cai, Y., & Li, S. (Eds.). (2019). *Computational Methods and Clinical Applications for Spine Imaging* (Vol. 11397). Springer International Publishing. https://doi.org/10.1007/978-3-030-13736-6

Zheng, G., Chu, C., Belavý, D. L., Ibragimov, B., Korez, R., Vrtovec, T., Hutt, H., Everson, R., Meakin, J., Andrade, I. L., Glocker, B., Chen, H., Dou, Q., Heng, P. A., Wang, C., Forsberg, D., Neubert, A., Fripp, J., Urschler, M., … Li, S. (2017). Evaluation and comparison of 3D intervertebral disc localization and segmentation methods for 3D T2 MR data: A grand challenge. *Medical Image Analysis*, *35*, 327–344. https://doi.org/10.1016/j.media.2016.08.005

Proposed Certificate for Plagiarism

It is certified that PhD/M.Phil/MS Thesis Titled **Intervertebral Disc Segmentation Using Machine Learning** by **Iqra Saeed** has been examined by us. We undertake the follows:

a. Thesis has significant new work/knowledge as compared already published or are under consideration to be published elsewhere. No sentence, equation, diagram, table, paragraph or section has been copied verbatim from previous work unless it is placed under quotation marks and duly referenced.

b. The work presented is original and own work of the author (i.e. there is no plagiarism). No ideas, processes, results or words of others have been presented as Author own work.

c. There is no fabrication of data or results which have been compiled/analyzed.

d. There is no falsification by manipulating research materials, equipment or processes, or changing or omitting data or results such that the research is not accurately represented in the research record.

e. The thesis has been checked using TURNITIN (copy of originality report attached) and found within limits as per HEC plagiarism Policy and instructions issued from time to time.

Name & Signature of Supervisor

__Dr. Syed Omer Gilani____

Signature: _____